Contribution from the Institut für Anorganische Chemie, Universität Bern, CH-3000 Bern 9, Switzerland, and Anorganisch-Chemisches Institut der Universität Zürich, CH-8057 Zürich, Switzerland

Electronic Properties of Hexaaquaruthenium(III): EPR and Optical Spectra of $Ru(H_2O)_6^{3+}$ in Alum Crystals

PAUL BERNHARD,*[1a] ANTON STEBLER,[1b] and ANDREAS LUDI[1a]

Received October 7, 1983

Powder susceptibility measurements on $CsRu(SO_4)_2 \cdot 12H_2O$ between 2.6 and 200 K yield a temperature-independent magnetic moment of 1.92 (1) μ_B with an average g of 2.22 (1). Powder and single-crystal electron paramagnetic spectra of $^{101}Ru(H_2O)_6^{3+}$ doped in $CsGa(SO_4)_2 \cdot 12H_2O$ have been measured at 3 K. The resonances are described by axial g tensors with principal axes parallel to ⟨111⟩. The components of the g tensor are $|g_\parallel| = 1.494$ (5) and $|g_\perp| = 2.517$ (5) ($\langle g^2 \rangle^{1/2} = 2.23$) with hyperfine coupling constants $|A_\parallel| = 0.0022$ (1) cm^{-1} and $|A_\perp| \approx 0.0001$ (1) cm^{-1}. Analysis of the EPR results with inclusion of spin–orbit coupling, trigonal field splitting, and electrostatic repulsion between the ground and excited $^2T_{2g}$ states gives $D_{trig}/\lambda = -0.35$ and $k = 0.91$ by using $10Dq = 30000$ cm^{-1}, $C/B = 4.0$, and $B = 600$ cm^{-1} as estimated from a single-crystal absorption spectrum of $CsRu(SO_4)_2 \cdot 12H_2O$ at 12 K.

Introduction

Only a rather few aqua ions have been thoroughly characterized within the second and third transition-metal series, in sharp contrast to the 3d metals. In particular, a well-defined redox couple has been described only for ruthenium. A few studies concerning the electronic structure of $Ru(H_2O)_6^{3+}$ with its low-spin d^5 configuration have been performed in dilute solutions including the measurement of the optical spectrum[2,3] and a determination of the magnetic susceptibility from ^1H NMR data.[4] A magnetic moment of 2.02–2.06 μ_B (278–329 K) and a spin–orbit coupling constant of 1200 (200) cm^{-1} have been reported.[4] Following the isolation of stable crystalline salts[5] of $Ru(H_2O)_6^{2+}$ and $Ru(H_2O)_6^{3+}$, we have initiated a comprehensive study of these aqua ions. The present paper discusses the electronic structure of $Ru(H_2O)_6^{3+}$ based on powder susceptibility data of $CsRu(SO_4)_2 \cdot 12H_2O$, powder and single-crystal EPR measurements of $^{101}Ru(H_2O)_6^{3+}$ doped into Cs–Ga–alum, and optical single-crystal spectroscopy on $CsRu(SO_4)_2 \cdot 12H_2O$.

Experimental Section

A. Sample Preparation. Ruthenium metal containing 93.1% ^{101}Ru and 5.7% ^{102}Ru (Medipro, CH-9053 Teufen, Switzerland) was used for the synthesis of $^{101}Ru(H_2O)_6(tos)_3 \cdot 3H_2O$ (tos = *p*-toluenesulfonate).[5] Single crystals of $CsRu(SO_4)_2 \cdot 12H_2O$ were grown by slow cooling or slow evaporation of an aqueous solution containing Cs_2SO_4, $Ru(H_2O)_6(tos)_3 \cdot 3H_2O$, and H_2SO_4 in stoichiometric proportions. Doped ^{101}Ru–Ga–alums were obtained by the analogous procedure using a saturated solution of $CsGa(SO_4)_2 \cdot 12H_2O$ containing 3% $^{101}Ru(H_2O)_6(tos)_3 \cdot 3H_2O$. Precession photographs verified that both the pure and the doped alums crystallize with {111} as main faces.

B. Spectroscopy. The single-crystal absorption spectrum (900–260 nm) of $CsRu(SO_4)_2 \cdot 12H_2O$ at 12 K was recorded on a Cary 17 spectrophotometer equipped with a special red-sensitive photomultiplier using a helium closed-cycle cryostat (Air Products). Crystal thickness varied from 0.2 to 0.8 mm. The incident beam was parallel to the trigonal axis of the crystal. Other orientations are not expected to give a different spectrum owing to the cubic symmetry of the crystal.

C. Magnetic Susceptibility. The powder susceptibility of $CsRu(SO_4)_2 \cdot 12H_2O$ (2.6–200 K) was measured at the Laboratorium für Festkörperphysik, ETH Zürich, by using the moving-sample technique.[6] At each temperature several measurements were taken checking thermal and magnetic equilibria. The temperature was measured to ±0.2 K with a chromel/gold–iron thermocouple. The susceptibility was calibrated with Ni powder (puriss.) and corrected for diamagnetic contributions.[7]

D. Electron Paramagnetic Resonance. EPR measurements were performed with a Varian E-109 X-band spectrometer. Microwave frequency and magnetic field were measured with an EIP 350 D frequency counter and a Varian NMR gaussmeter, respectively. The spectra were recorded at 3 K by using an EPR-10 helium flow cryostat (Oxford Instruments) with a VC 30 variable-temperature controller unit. A goniometer was employed to rotate the crystal inside the cavity about the vertical axis. Single-crystal ($\approx 3 \times 3 \times 2$ mm^3) measurements were performed on $CsGa(SO_4)_2 \cdot 12H_2O$ doped with 3% $^{101}Ru(H_2O)_6^{3+}$. Spectra were recorded with rotation about the [110] and the [111] axes. The final crystal orientation in the cavity was found to be correct within ±4°.

Theoretical Formalism

In low-spin d^5 complexes the unpaired electron occupies the t_{2g} orbitals, which are split under the combined effects of noncubic ligand fields and spin–orbit coupling. The problem can be reduced to that of a single hole in the t_{2g} orbitals and can be treated as the d^1 configuration[8] (as long as interactions with excited configurations are neglected) with change of sign for the spin–orbit coupling constant λ and the low-symmetry field parameter D. Analytical expressions for $|g_\parallel|$ and $|g_\perp|$ considering spin–orbit coupling, trigonal field splitting, and Zeeman interaction with a magnetic field using trigonally quantized d orbitals[9] within the hole formalism are derived. We adopt the formalism and nomenclature of Abragam and Bleaney's textbook.[10] The influence of excited configurations will be estimated subsequently.

From the T_{2g}–P analogy for the effective angular momentum quantum number ($L = 1$) the wave functions are[10]

$$|\tilde{0}\rangle = |0\rangle \qquad |+\tilde{1}\rangle = 1/3^{1/2}|+1\rangle - (^2/_3)^{1/2}|-2\rangle$$
$$|-\tilde{1}\rangle = -1/3^{1/2}|-1\rangle + (^2/_3)^{1/2}|+2\rangle \tag{1}$$

In this basis set, operators containing $\hat{L}$ change sign:

$$\hat{H} = \hat{H}_{s.o.} + \hat{H}_{trig} + \hat{H}_{ze}$$
$$= \lambda \hat{L}_z \hat{S}_z + \lambda(\hat{L}_+ \hat{S}_- + \hat{L}_- \hat{S}_+)/2 - D(\hat{L}_z^2 - {}^2/_3) + \sum_i (-K\hat{L}_i + 2\hat{S}_i)\beta H_i \quad (i = x, y, z) \tag{2}$$

where all required changes of sign have been introduced. The corresponding matrix is given in Table I. At zero magnetic field the eigenvalues and eigenfunctions of the three Kramers doublets are

$$E_1,E_2: \ -D/3 + \lambda/2 \qquad \Psi_1: \ |+\tilde{1}^+\rangle \qquad \Psi_2: \ |-\tilde{1}^-\rangle$$
$$E_3,E_4: \ (D/3 - \lambda/2)/2 + (D^2 + D\lambda + 9\lambda^2/4)^{1/2}/2$$
$$\Psi_3: \ \cos\delta|-\tilde{1}^+\rangle - \sin\delta|\tilde{0}^-\rangle \qquad \Psi_4: \ \cos\delta|+\tilde{1}^-\rangle - \sin\delta|\tilde{0}^+\rangle \tag{3}$$
$$E_5,E_6: \ (D/3 - \lambda/2)/2 - (D^2 + D\lambda + 9\lambda^2/4)^{1/2}/2$$
$$\Psi_5: \ \sin\delta|-\tilde{1}^+\rangle + \cos\delta|\tilde{0}^-\rangle \qquad \Psi_6: \ \sin\delta|+\tilde{1}^-\rangle + \cos\delta|\tilde{0}^+\rangle$$

where $\tan(2\delta) = 2^{1/2}/(D/\lambda + 0.5)$. These results are thus formally

(1) (a) Universität Bern. (b) Universität Zürich.
(2) Kallen, T. W.; Earley, J. E. *Inorg. Chem.* **1971**, *10*, 1149.
(3) Harzion, Z.; Navon, G. *Inorg. Chem.* **1980**, *19*, 2236.
(4) Harzion, Z.; Navon, G. *Inorg. Chem.* **1982**, *21*, 2606.
(5) Bernhard, P.; Bürgi, H. B.; Hauser, J.; Lehmann, H.; Ludi, A. *Inorg. Chem.* **1982**, *21*, 3936.
(6) Rebouillat, J. P. Thesis, CNRS, Grenoble, 1972.
(7) Landolt-Börnstein, "Physikalische und Chemische Tabellen"; Springer-Verlag: West Berlin, 1976; Neue Serie, Vol. II/8, pp 27–29.
(8) Bleaney, B.; O'Brien, M. C. M. *Proc. Phys. Soc., London Sect. B* **1956**, *B69*, 1216.
(9) Tanabe, Y.; Sugano, S.; Kamimura, H. "Multiplets of Transition Metal Ions in Crystals"; Academic Press: New York, London, 1972.
(10) Abragam, A.; Bleaney, B. "Electron Paramagnetic Resonance of Transition Ions"; Clarendon Press: Oxford, 1976.

0020-1669/84/1323-2151$01.50/0

Table I. Perturbation Matrix of $^2T_{2g}$ in Hole Formalism[a]

	$\|+\tilde{1}^+\rangle$	$\|+\tilde{1}^-\rangle$	$\|\tilde{0}^+\rangle$	$\|\tilde{0}^-\rangle$	$\|-\tilde{1}^+\rangle$	$\|-\tilde{1}^-\rangle$
$\langle+\tilde{1}^+\|$	$-D/3 + \lambda/2 + (1-k)\beta H_z$	$+\beta H^-$	$-k\beta H^-/2^{1/2}$			
$\langle+\tilde{1}^-\|$	$+\beta H^+$	$-D/3 - \lambda/2 - (1+k)\beta H_z$	$+\lambda/2^{1/2}$	$-k\beta H^-/2^{1/2}$		
$\langle\tilde{0}^+\|$	$-k\beta H^+/2^{1/2}$	$+\lambda/2^{1/2}$	$+2D/3 + \beta H_z$	$+\beta H^-$	$-k\beta H^-/2^{1/2}$	
$\langle\tilde{0}^-\|$		$-k\beta H^+/2^{1/2}$	$+\beta H^+$	$+2D/3 - \beta H_z$	$+\lambda/2^{1/2}$	$-k\beta H^-/2^{1/2}$
$\langle-\tilde{1}^+\|$			$-k\beta H^+/2^{1/2}$	$+\lambda/2^{1/2}$	$-D/3 - \lambda/2 + (1+k)\beta H_z$	$+\beta H^-$
$\langle-\tilde{1}^-\|$				$-k\beta H^+/2^{1/2}$	$+\beta H^+$	$-D/3 + \lambda/2 - (1-k)\beta H_z$

[a] $H^+ = H_x + iH_y; H^- = H_x - iH_y$.

Table II. Matrix Elements between $|t_2^5\,{}^2T_2\rangle$ and $|t_2^4({}^3T_1)e\,{}^2T_2\rangle$[a]

	t_2^5					
t_2^4e	$\|+1^+\rangle$	$\|+1^-\rangle$	$\|0^+\rangle$	$\|0^-\rangle$	$\|-1^+\rangle$	$\|-1^-\rangle$
$\langle+1^+\|$	$-3(6^{1/2})B - \lambda/(2(6^{1/2})) + (3/2)^{1/2}kH_z$		$+3^{1/2}kH^-/2$			
$\langle+1^-\|$		$-3(6^{1/2})B + \lambda/(2(6^{1/2})) + (3/2)^{1/2}kH_z$	$-3^{1/2}\lambda/6$	$+3^{1/2}kH^-/2$		
$\langle0^+\|$	$+3^{1/2}kH^+/2$	$-3^{1/2}\lambda/6$	$-3(6^{1/2})B$		$+3^{1/2}kH^-/2$	
$\langle0^-\|$		$+3^{1/2}kH^+/2$		$-3(6^{1/2})B$	$-3^{1/2}\lambda/6$	$+3^{1/2}kH^-/2$
$\langle-1^+\|$			$+3^{1/2}kH^+/2$	$-3^{1/2}\lambda/6$	$-3(6^{1/2})B + \lambda/(2(6^{1/2})) - (3/2)^{1/2}kH_z$	
$\langle-1^-\|$				$+3^{1/2}kH^+/2$		$-3(6^{1/2})B - \lambda/(2(6^{1/2}) - (3/2)^{1/2}kH_z$

[a] $H^+ = H_x + iH_y; H^- = H_x - iH_y$.

identical with those for a d^1 configuration with a tetragonal[11] or a trigonal distortion. However, the Kramers doublet belonging to E_5,E_6 is lowest (for d^1: E_3,E_4), well separated from the other two doublets. Diagonalization of the Zeeman perturbation within the ground doublets leads to the following components of the **g** tensor:

$$|g_\parallel| = 2\cos(2\delta) - K(1 - \cos(2\delta))$$
$$|g_\perp| = 1 + \cos(2\delta) - 2^{1/2}K\sin(2\delta) \quad (4)$$

K can be considered as an apparent orbital reduction factor of the t_{2g}^5 configuration including contributions from interactions with excited configurations but is not a measure of delocalization or covalency. Diagonalization of the electrostatic matrices of the ground and $^2T_{2g}$ states arising from the singly and the doubly excited configuration with $10Dq = 30\,000$ cm^{-1}, $C/B = 4.0$, and $B = 600$ cm^{-1} (vide infra) gives the ground-state wave function

$$|{}^2T_{2g}\rangle = 0.99|t_2^5\,{}^2T_2\rangle - 0.11|t_2^4({}^3T_1)e\,{}^2T_2\rangle + 0.002|t_2^4({}^1T_2)e\,{}^2T_2\rangle + \ldots + 0.09|t_2^3({}^2T_2)e^2({}^3A_1)\,{}^2T_2\rangle + \ldots \quad (5)$$

where all excited states except $|t_2^4({}^3T_1)e\,{}^2T_2\rangle$ may be neglected since the angular momentum operator $k\hat{L}_i$ has no matrix elements between the ground and doubly excited states and the coefficient of $|t_2^4({}^1T_2)e\,{}^2T_2\rangle$ is small. The matrix elements between the two states are given in Table II. Determinental wave functions introduced by Griffith[12] have been used. Wave functions for the excited state are found by combining the $^3T_1$ functions with the E functions. The general matrix element of the operator $k\hat{L}_i$ is

$$({}^2T_{2g})\langle M_s M_{L_1}|k\hat{L}_i|M_s M_{L_2}\rangle = (t_2^5)\langle M_s M_{L_1}|\hat{L}_i|M_s M_{L_2}\rangle k(1 + 2(0.11)(0.99)(3/2)^{1/2}) \quad (6)$$

on the assumption that k has the same value for the t_{2g}^5 and the t_{2g}^4e configurations. The orbital reduction in the t_{2g}^5 configuration is therefore $k = K/1.267$. This result compares well with the general approximation by Hill[13] (eq 7) where E is the mean energy difference between the ground and the two singly excited $^2T_{2g}$ states.

$$k = K/(1 + 12B/E) = K/1.222 \quad (7)$$

Results and Discussion

A. Crystal Structure. The crystal structure of a series of Cs alums including $CsGa(SO_4)_2\cdot 12H_2O$ have been discussed recently.[14] The alums are cubic with space group $Pa3$ with 4 formula units per unit cell. They exist in three types termed α, β, and γ depending on small differences in atomic arrangements. Since the crystal shape of $CsRu(SO_4)_2\cdot 12H_2O$ corresponds well to those described for other Cs alums,[15] we assume the β-type structure for the Cs–Ru–alum for which the unit cell dimension is 12.447 (4) Å.[16] X-ray data[14] show the β-alums to contain almost regular $M(H_2O)_6^{3+}$ octahedra; their cubic axes are directed along the axes of the crystal. The ⟨111⟩ axes thus coincide with the threefold axes of the $Ru(H_2O)_6^{3+}$ octahedron with site symmetry $S6$.

B. Spectroscopy. The absorption spectrum (Figure 1) shows a weak broad band at 18 000 cm^{-1} and a distinct absorption at 26 600 cm^{-1}, which are attributed to the spin-forbidden $^2T_{2g} \rightarrow {}^4T_{1g}$ and spin-allowed $^2T_{2g} \rightarrow {}^2T_{1g},{}^2A_{2g}$ transitions, respectively. Additional bands might be hidden under the tail of the intense charge-transfer band at 44 000 cm^{-1}.[3] The

(11) Wertz, J. E.; Bolton, J. R. "Electron Spin Resonance"; Mc Graw-Hill: New York, 1972.
(12) Griffith, J. S. "The Theory of Transition Metal Ions"; Cambridge University Press: New York, 1961.
(13) Hill, J. N. *J. Chem. Soc., Faraday Trans. 2* **1972**, 427.
(14) Beattie, J. K.; Best, S. P.; Skelton, B. W.; White, A. H. *J. Chem. Soc., Dalton Trans.* **1981**, 2105.
(15) Haussühl, S. *Z. Kristallogr., Kristallgeom., Kristallphys., Kristallchem.* **1961**, *116*, 371.
(16) Bernhard, P.; Ludi, A. *Inorg. Chem.* **1984**, *23*, 870.

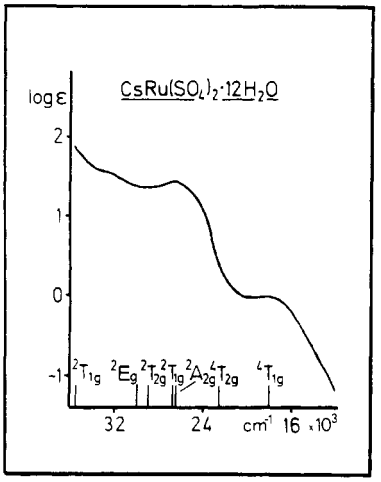

Figure 1. Single-crystal absorption spectrum of $CsRu(SO_4)_2 \cdot 12H_2O$ at 12 K. Transitions are calculated with $10Dq = 30\,000$ cm^{-1}, $B = 600$ cm^{-1}, and $C/B = 4.0$.

Table III. Absorption Bands and Crystal Field Parameters for $Ru(H_2O)_6^{3+}$

$^2T_{2g} \rightarrow {}^4T_{1g}$: 18 000 (400) cm^{-1}
$^2T_{2g} \rightarrow {}^2A_{2g}, {}^2T_{1g}$: 26 600 (200) cm^{-1}

	$C/B = 3.5$	$C/B = 4.0$	$C/B = 4.5$
$10D_q$, cm^{-1}	30 030 (200)	30 000 (200)	29 910 (200)
B, cm^{-1}	660 (40)	600 (40)	540 (40)

absorption bands of the crystal occur at higher energy (1000–1500 cm^{-1}) than the corresponding bands in the solution spectrum owing to an increase of Dq at low temperature. Our data are not sufficient to independently determine Dq, B, and C. Table III summarizes the results fitting the spectrum with various sets of parameters by diagonalization of the Tanabe–Sugano matrices.[9] Values of $10Dq$ cluster around 30 000 cm^{-1}, whereas B depends on the C/B ratio. Transition energies in Figure 1 are calculated by using $10Dq = 30\,000$ cm^{-1}, $B = 600$ cm^{-1}, and $C/B = 4.0$.

C. Magnetic Susceptibility. The paramagnetic susceptibility of a $CsRu(SO_4)_2 \cdot 12H_2O$ powder obeys the Curie law from 2.6 to 200 K (Figure 2). A fit of the experimental values to the Curie–Weiss equation (eq 8) gives the parameters $C = 0.463$

$$\chi_M = C/(T + \Theta) \quad (8)$$

(1) emu·K·mol^{-1} and $\Theta = 0.209$ (3) K from which an average g of 2.22 (1) and a temperature-independent magnetic moment of 1.92 (1) μ_B are calculated. The temperature independence of the effective magnetic moment indicates that the combined action of spin–orbit coupling and low symmetry field splitting must be considered although no precise information on the spin–orbit coupling constant and the low symmetry field parameter can be obtained from these results.

D. Electron Paramagnetic Resonance. From an X-band powder spectrum of 3% $^{101}Ru(H_2O)_6^{3+}$ doped in $CsGa(SO_4)_2 \cdot 12H_2O$ (Figure 3) an axial **g** tensor with principal values of $|g_\parallel| = 1.489$ (5) and $|g_\perp| = 2.514$ (5) is obtained. The symmetry of the **g** tensor clearly shows that the $Ru(H_2O)_6^{3+}$ octahedron is distorted. Moreover, a hyperfine coupling of the electron spin with the ^{101}Ru nucleus ($I = {}^5/_2$) producing six equally spaced lines with $|A_\parallel| = 0.0022$ cm^{-1} is observed. The incompletely resolved central lines reveal the presence of an additional unsplit signal arising from ^{102}Ru ($I = 0$). The average $\langle g^2 \rangle^{1/2}$ of 2.23 corresponds well with the value obtained from the susceptibility measurement.

The angular dependence of the g values of a ^{101}Ru-doped alum crystal rotated about the [110] axis is shown in Figure 4. In β-alums the **g** tensors of the four crystallographically

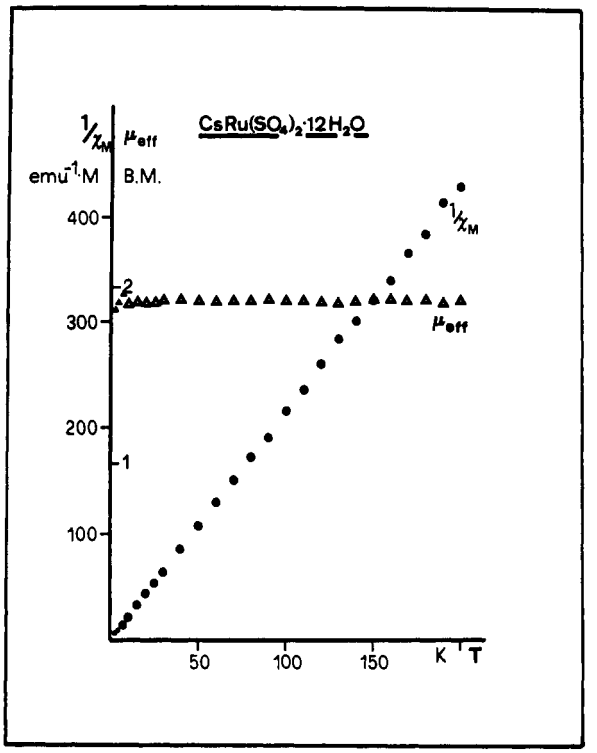

Figure 2. Plot of $1/\chi_M$ and μ_{eff} vs. temperature for $CsRu(SO_4)_2 \cdot 12H_2O$.

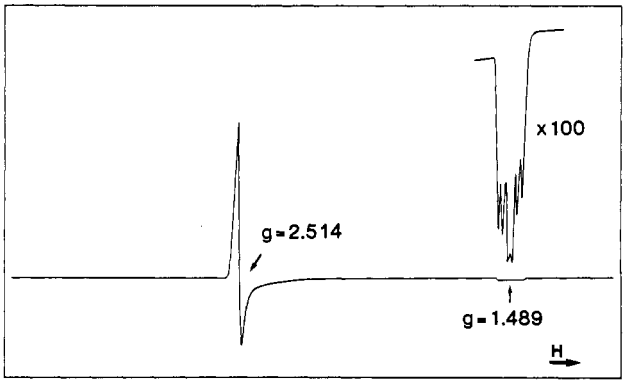

Figure 3. EPR spectrum of a polycrystalline sample of 3% $^{101}Ru(H_2O)_6^{3+}$ doped in $CsGa(SO_4)_2 \cdot 12H_2O$ at 3 K.

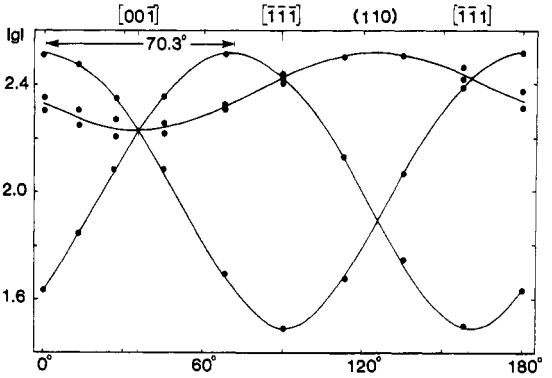

Figure 4. Angular dependence of the g value of a single crystal of 3% $^{101}Ru(H_2O)_6^{3+}$ in $CsGa(SO_4)_2 \cdot 12H_2O$ rotated about the [110] axis at 3 K.

equivalent $M(H_2O)_6^{3+}$ octahedra show different orientations. When the single crystal is rotated about the [110] axis, not more than three resonances should appear. From Figure 4 it is evident that the coincidence of two resonances is removed due to a small misalignment of the crystal (±4°). The reso-

Table IV. g and A Tensors of Low-Spin d^5 Ions in Various Host Lattices

guest	host		$\|g_x\|$	$\|g_y\|$	$\|g_z\|$	$\|A_x\|^a$	$\|A_y\|^a$	$\|A_z\|^a$	ref
$Ru(H_2O)_6^{3+}$	$CsGa(SO_4)_2 \cdot 12H_2O$		2.517 (5)		1.494 (5)		1 (1)	22 (1)	this work
$Ru(NH_3)_6^{3+}$	$Co(NH_3)_6Cl_3$ [b]	I	2.06 (1)	2.02 (1)	1.72 (1)	48 (2)	48 (2)	49 (2)	
		II	1.80 (1)	1.90 (1)	2.06 (1)	48 (2)	48 (2)	50 (2)	22, 23
		III	1.15 (1)	1.84 (1)	2.66 (1)	45 (2)	41 (2)	54 (2)	
Ru^{3+}	Al_2O_3		2.430		<0.06		43		18
$RuCl_6^{3-}$	Cs_2HfCl_6			1.904	isotropic		50.2 (1)	isotropic	21
$RuCl_6^{3-}$	Na_3RuCl_6			2.10 (1)	isotropic		26 (2)	isotropic	24
$Mn(CN)_6^{4-}$	$K_4Fe(CN)_6 \cdot 3H_2O$		2.624 (8)	2.182 (8)	0.63	85.5 (5)	46.5 (5)	104 (20)	8
$IrCl_6^{2-}$	$Na_2PtCl_6 \cdot 6H_2O$		2.168 (5)	2.078 (5)	1.050	26 (1)	26 (1)	24.9 (5)	25
$IrCl_6^{2-}$	$(NH_4)_2PtCl_6$			1.786 (4)	isotropic		26.3 (6)	isotropic	

[a] In units of 10^{-4} cm^{-1}. [b] Contains three pairs of magnetically inequivalent complexes.

nances are described by four axial **g** tensors that have their unique axes along the ⟨111⟩ directions. The angle between the principal axes of any two sites is 70.3°, which is in very good agreement with the angle of 70.5° defined by symmetry. The g values are $|g_\parallel| = 1.500$ (5) and $|g_\perp| = 2.519$ (5). These results were verified by a second experiment in which the single crystal was rotated about the [111] axis. The site having the unique axis parallel to the rotation axis always shows an isotropic value of $|g_\perp|$. The angle between the maximum value of the three remaining **g** tensors is 60°.

Additional weak resonance lines in the crystal spectra are attributed to some paramagnetic impurity (probably Mn^{2+}). The possibility of the presence of high-spin $Ru(H_2O)_6^{3+}$ can be ruled out because the $^6A_{1g}$ state lies about 27 000 cm^{-1} above the ground $^2T_{2g}$ state.

The experimental values can be best fitted to the Hamiltonian (eq 2) with $D_{trig}/\lambda = -0.35$ and $K = 1.15$. In order to calculate the absolute magnitude of D_{trig}, the spin–orbit coupling constant should be known. The spin–orbit coupling constant for the free Ru^{3+} ion has been reported to be 1197 cm^{-1}.[17] We adopt $\lambda = 1000$ cm^{-1} as a reasonable estimate for $Ru(H_2O)_6^{3+}$, giving a trigonal splitting parameter of −350 cm^{-1}. The following eigenvalues for the three Kramers doublets are obtained: $E_5,E_6 = -1010.4$ cm^{-1}; $E_3,E_4 = 402.7$ cm^{-1}; $E_1,E_2 = 616.6$ cm^{-1}.

With $K = 1.15$ the orbital reduction in the t_{2g}^5 configuration is given by $k = K/1.267 = 0.91$ (Hill (eq 7): 0.93). For Ru^{3+} doped in Al_2O_3 an uncorrected $K = 0.837$ has been reported.[18]

Only the resonance at high field is split by hyperfine interactions in the crystal as well as in the powder spectrum. The line width of $|g_\perp|$ is about the same as the hyperfine coupling constant $|a_\parallel|$ (≈31 G); therefore, $|a_\perp|$ must be considerably smaller than $|a_\parallel|$. The analytical expression

$$(g \cdot A)_{eff}^2 = (g_\parallel \cdot A_\parallel)^2 \cos^2\theta + (g_\perp \cdot A_\perp)^2 \sin^2\theta \qquad (9)$$

gives (cf. Figure 5) $|A_\parallel| = 0.0022$ (1) cm^{-1} and $|A_\perp| = 0.0001$ (1) cm^{-1}. For the purpose of comparison, Table IV contains a collection of hyperfine coupling constants reported for Ru(III) compounds.

The hyperfine splitting is expected to increase going from the 3d to the 4d (and 5d) ions because the amplitude of the wave function near the nucleus increases with Z. It also depends upon the nuclear magnetic moment, however, which is the main reason why the splitting for $^{101}Ru(H_2O)_6^{3+}$ ($\mu_N = -0.69$ NM)[10] is smaller than for $^{55}Mn(CN)_6^{4-}$ ($\mu_N = 3.44$ NM).[8,10] In the case of octahedral Ir^{4+} ($5d^5$) for which about the same hyperfine constants are obtained as for $Ru(H_2O)_6^{3+}$, the nuclear magnetic moment is even lower and the spin–dipolar contribution vanishes, which may outweigh the increase in $\langle r^{-3} \rangle$, the average value of the radial wave function of the t_{2g} electrons, and in χ, the density of unpaired spins at the nucleus. The hyperfine splitting constants for $Ru(H_2O)_6^{3+}$

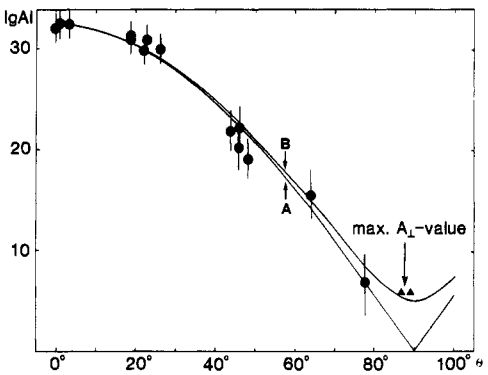

Figure 5. $|g \cdot A|$ values (●) of 3% $^{101}Ru(H_2O)_6^{3+}$ in $CsGa(SO_4)_2 \cdot 12H_2O$ as a function of θ, the angle between g and the unique tensor axis: trace A, $|A_\parallel| = 0.0022$ cm^{-1} and $|A_\perp| = 0$; trace B, $|A_\parallel| = 0.0022$ cm^{-1} and $|A_\perp| = 0.0002$ cm^{-1} (eq 9). The maximum value of $|A_\perp|$ (▲) is estimated from the line width of $|g_\perp|$.

are reduced by at least a factor of 2 compared to those for $Ru(NH_3)_6^{3+}$ (Table IV). This can be partly explained by a $p\pi$–$d\pi$ interaction between one lone pair of the oxygen atom and the metal t_{2g} orbital, thus spreading out the spin density onto the ligands, an interaction that is not possible for $Ru(NH_3)_6^{3+}$. This interaction[19] is illustrated by comparing the corresponding metal to ligand distances, 2.03 Å in $Ru(H_2O)_6^{3+}$[5] vs. 2.10 Å in $Ru(NH_3)_6^{3+}$.[20]

It is difficult to say whether orbital, spin–dipolar interaction, or core polarization contributes most to the hyperfine splitting. It has been suggested[10] that for Ru^{3+} doped in $Co(NH_3)_6Cl_3$ core polarization is the most important mechanism since the splitting has remarkably constant values regardless of the symmetry of the **g** tensor. In the case of $Ru(H_2O)_6^{3+}$ the anisotropic **g** and **A** tensors indicate that the orbital and/or spin–dipolar contribution must be important. The latter contribution is probably small owing to the high symmetry of $Ru(H_2O)_6^{3+}$. An upper limit of the isotropic contribution to the hyperfine splitting is given by the average of the trace of the **A** tensor (≈0.0008 cm^{-1}). For this reason, the contamination of the ground state with excited configurations containing unpaired s electrons and core polarization are expected to be smaller than for $Ru(NH_3)_6^{3+}$.

An important result of this study is the observed temperature independence of the effective magnetic moment of $CsRu(SO_4)_2 \cdot 12H_2O$, a unique feature for low-spin d^5 compounds. Our detailed analysis of the EPR spectra of $^{101}Ru(H_2O)_6^{3+}$ con-

(17) Blume, M.; Freeman, A. J.; Watson, R. E. *Phys. Rev.* **1964**, *134*, A320.
(18) Gschwind, S.; Remeika, J. P. *J. Appl. Phys.* **1962**, *33*, 370.
(19) Böttcher, W.; Brown, G. M.; Sutin, N. *Inorg. Chem.* **1979**, *18*, 1447.
(20) Stynes, H. C.; Ibers, J. A. *Inorg. Chem.* **1971**, *10*, 2304.
(21) Maniv, S.; Gabay, A. *J. Magn. Reson.* **1974**, *13*, 148.
(22) Griffiths, J. H. E.; Owen, J.; Ward, R. *Proc. R. London, Ser. A* **1953**, *A219*, 526.
(23) Griffiths, J. H. E.; Owen, J.; Ward, R.; O'Brien, M. C. M. *Rep. Prog. Phys.* **1955**, *18*, 304.
(24) Abdrakhmanov, R. S.; Garif'yanov, N. S.; Semenova, E. I. *Russ. J. Inorg. Chem.* (*Engl. Transl.*) **1972**, *17*, 613.
(25) Thornley, J. H. M. *J. Phys. C* **1968**, *1*, 1024.

clusively reveals a corresponding strong axial anisotropy of the g tensor in agreement with the trigonal site symmetry in the alum lattice. A pronounced anisotropy is also observed for the A tensor indicative of the importance of orbital contributions to the hyperfine interaction.

Acknowledgment. We thank K. Mattenberger, Laboratorium für Festkörperphysik, ETH Zürich, for the measurement of the powder susceptibility and the Swiss National Science Foundation for financial support (Grants 2.209.-0.81 and 2.442.-0.82).

Registry No. $CsRu(SO_4)_2 \cdot 12H_2O$, 88703-99-5; $CsGa(SO_4)_2 \cdot 12H_2O$, 13530-72-8; $Ru(H_2O)_6^{3+}$, 30251-72-0.

Contribution from the Department of Chemistry, State University of New York at Binghamton, Binghamton, New York 13901

Photophysics of Metal Carbonyl Complexes. Excited States of a Series of *cis*-$M(CO)_4L_2$ Complexes (M = Cr, Mo, or W; L = Pyridine or a Pyridine Derivative)[1]

SAMUEL CHUN, EDWARD E. GETTY, and ALISTAIR J. LEES*

Received November 28, 1983

Electronic absorption and emission spectra at 298 K are reported for a series of *cis*-$M(CO)_4L_2$ complexes, where M = Cr, Mo, or W and L = 4-ethylpyridine, 4-methylpyridine, pyridine, 4-phenylpyridine, 3,5-dichloropyridine, 4-benzoylpyridine, or 4-cyanopyridine. Low-lying ligand-field (LF) and metal to ligand charge-transfer (MLCT) transitions are observed in the electronic absorption spectra. The emission centered in the 550–700-nm region is sensitive to the nature of ligand substituent and solvent and for each complex is assigned to originate from the low-energy MLCT state. Emission quantum yields vary greatly with ligand substituent and range from 0.1×10^{-4} to 56×10^{-4}. Photosubstitution quantum yields of *cis*-$W(CO)_4L_2$ complexes are markedly affected by changes in the ligand substituent and excitation wavelength. The low-lying MLCT state is virtually unreactive toward ligand substitution, whereas the higher energy LF state has substantially higher photoreactivity. The spectral and photochemical data lead us to assign that, for L = 4-ethylpyridine, 4-methylpyridine, or pyridine, the LF and MLCT states are approximately at the same energy whereas, for L = 4-phenylpyridine, 3,5-dichloropyridine, 4-benzoylpyridine, and 4-cyanopyridine, the MLCT state is clearly the lowest energy transition. An excited-state scheme based on the experimental observations is presented.

Introduction

There has been considerable interest in the photochemistry of transition-metal complexes that have low-lying metal to ligand charge-transfer (MLCT) excited states. For example, $Ru(NH_3)_5L^{2+}$,[2] $W(CO)_5L$,[3-7] $(\eta^5\text{-}C_5H_5)Re(CO)_2L$,[8] $(\eta^5\text{-}C_5H_5)Mn(CO)_2L$,[8] and $Fe(CN)_5L$[9] complexes, where L is CO or a nitrogen, oxygen, or phosphorus donor, have been extensively studied. The results of these studies have shown that the luminescence and photochemical characteristics of the complexes are dependent on the relative position of the low-lying MLCT excited state. Small changes in the nature of the ligand (L) can have a major effect on the properties of the complex; therefore, the ligand substituent can be used to "tune" the excited states and the photochemical properties of transition metal complexes.[10]

Most investigations of the emissive properties of transition-metal complexes have been carried out at low temperature in a rigid environment, where nonradiative deactivation processes are considerably reduced.[11] As a consequence there are relatively few examples of luminescence from metal complexes in fluid solution, but when such cases are found, valuable information on excited-state processes can be obtained.[12,13] Metal carbonyl complexes in particular have not been considered to be emissive in fluid solution due to the relatively high photoreactivity and efficient nonradiative rates of their excited states. Several $ClRe(CO)_3L$ complexes, where L = 1,10-phenanthroline and related ligands, have been observed to emit in solution.[14] The emission from these complexes was inferred to originate from a low-lying MLCT excited state and to have substantial triplet character. The emission was observed to be remarkably sensitive to the nature of the environment, yielding a red-orange emission in fluid solution at 298 K and a yellow-green emission in rigid glasses at 77 K.[14b] Emission at 298 K has also been reported from a series of $XRe(CO)_3L_2$ complexes, where X = Cl, Br, or I and L =

(1) Reported in part at the 13th Northeast Regional Meeting of the American Chemical Society, Hartford, CT, June 1983; see Abstracts, No. INORG/ORG PHOTOCHEM 102.
(2) (a) Ford, P.; Rudd, D. P.; Gaunder, R.; Taube, H. *J. Am. Chem. Soc.* **1968**, *90*, 1187. (b) Ford, P. C.; Stuermer, D. H.; McDonald, D. P. *Ibid.* **1969**, *91*, 6209. (c) Chaisson, D. A.; Hintze, R. E.; Stuermer, D. H.; Petersen, J. D.; McDonald, D. P.; Ford, P. C. *Ibid.* **1972**, *94*, 6665. (d) Malouf, G.; Ford, P. C. *Ibid.* **1974**, *96*, 601. (e) Hintze, R. E.; Ford, P. C. *Inorg. Chem.* **1975**, *14*, 1211. (f) Malouf, G.; Ford, P. C. *J. Am. Chem. Soc.* **1977**, *99*, 7213. (g) Matsubara, T.; Ford, P. C. *Inorg. Chem.* **1978**, *17*, 1747.
(3) (a) Wrighton, M.; Hammond, G. S.; Gray, H. B. *J. Am. Chem. Soc.* **1971**, *93*, 4336. (b) Wrighton, M.; Hammond, G. S.; Gray, H. B. *Inorg. Chem.* **1972**, *11*, 3122. (c) Wrighton, M.; Hammond, G. S.; Gray, H. B. *Mol. Photochem.* **1973**, *5*, 179. (d) Wrighton, M. S.; Abrahamson, H. B.; Morse, D. L. *J. Am. Chem. Soc.* **1976**, *98*, 4105.
(4) Frazier, C. C.; Kisch, H. *Inorg. Chem.* **1978**, *17*, 2736.
(5) (a) Dahlgren, R. M.; Zink, J. I. *Inorg. Chem.* **1977**, *16*, 3154. (b) Dahlgren, R. M.; Zink, J. I. *Ibid.* **1979**, *18*, 597. (c) Dahlgren, R. M.; Zink, J. I. *J. Am. Chem. Soc.* **1979**, *101*, 1448.
(6) (a) Schwenzer, G.; Darensbourg, M. Y.; Darensbourg, D. J. *Inorg. Chem.* **1972**, *11*, 1967. (b) Darensbourg, D. J.; Murphy, M. A. *Ibid.* **1978**, *17*, 884.
(7) (a) Boxhoorn, G.; Shoemaker, G. C.; Stufkens, D. J.; Oskam, A.; Rest, A. J.; Darensbourg, D. J. *Inorg. Chem.* **1980**, *19*, 3455. (b) Boxhoorn, G.; Oskam, A.; Gibson, E. P.; Narayanaswamy, R.; Rest, A. J. *Ibid.* **1981**, *20*, 783. (c) Boxhoorn, G.; Oskam, A.; McHugh, T. M.; Rest, A. J. *Inorg. Chim. Acta* **1980**, *44*, L1.
(8) Giordano, P. J.; Wrighton, M. S. *Inorg. Chem.* **1977**, *16*, 160.
(9) Figard, J. E.; Petersen, J. D. *Inorg. Chem.* **1978**, *17*, 1059.
(10) Ford, P. C. *Rev. Chem. Intermed.* **1979**, *2*, 267.
(11) Calvert, J. G.; Pitts, J. N. "Photochemistry"; Wiley-Interscience: New York, 1966; p 240.
(12) Fleischauer, P. D.; Fleischauer, P. *Chem. Rev.* **1970**, *70*, 199.
(13) Porter, G. B. "Concepts of Inorganic Photochemistry"; Adamson, A. W., Fleischauer, P. D., Eds.; Wiley-Interscience: New York, 1975; p 37.
(14) (a) Fredericks, S. M.; Luong, J. C.; Wrighton, M. S. *J. Am. Chem. Soc.* **1979**, *101*, 7415. (b) Wrighton, M.; Morse, D. L. *Ibid.* **1974**, *96*, 998. (c) Giordano, P. J.; Fredericks, S. M.; Wrighton, M. S.; Morse, D. L. *Ibid.* **1978**, *100*, 2257. (d) Luong, J. C.; Faltynek, R. A.; Wrighton, M. S. *Ibid.* **1979**, *101*, 1597.

0020-1669/84/1323-2155$01.50/0